Broadband Cloaking in Stratified Seas

Mohammad-Reza Alam[1]

[1]Department of Mechanical Engineering, University of California, Berkeley, California 94720, USA

(Received 13 September 2011; published 23 February 2012)

Here we show that floating objects in stratified fluids can be cloaked against broadband incident waves by properly architecting the bottom corrugations. The presented invisibility cloaking of gravity waves is achieved utilizing a nonlinear resonance concept that occurs between surface and internal waves mediated by the bottom topography. Our cloak bends wave rays from the surface into the body of the fluid. Wave rays then pass underneath the floating object and may be recovered back to the free surface at the downstream bearing no trace of diffraction or scattering. The cloak is the proper architecture of bottom corrugations only, and hence is surface noninvasive. The presented scheme is a nonlinear alternative to the transformation-based cloaking, but in the context of dispersive waves.

DOI: 10.1103/PhysRevLett.108.084502 PACS numbers: 47.35.Bb, 47.11.Kb, 47.20.Ma, 47.55.Hd

The density of water in an ocean or a sea is typically not constant. The variation of density is due to, mainly, variations of temperature and salinity. Solar radiation heats up the upper layer of the water, and the flow of rivers and the melting of ice lower the water density near the surface. Over time these effects add up to form a stable density stratification with the lighter fluid on top and the denser fluid below it. Stratified waters, besides regular surface waves, admit the so-called internal waves, which are gravity waves that propagate within the body of the water [1].

Field observations have reported ubiquitously nonuniform vertical gradient of stratification in the oceans: water density is nearly constant in an upper layer and then jumps, over a (relatively) thin horizontal plane of sudden density change—the so-called thermocline—, to a denser lower layer fluid. Density stays almost constant below the thermocline to the ocean floor (e.g., [2]). Therefore, for ocean scenarios a two-layer model, with the density of each layer constant within the layer, is plausible and widely used. If a two-layer density stratification assumption is employed, internal waves are restricted to propagate on the thermocline only. These waves, sometimes also called interfacial waves, are widely observed in the oceans, seas, and lakes [1,3–5].

Here we present the formation of a resonance between surface waves and interfacial waves caused by the physics of inhomogeneity (stratification) of ocean waters, the dispersive nature of gravity waves, and the nonlinearity of equations governing the motion of a fluid. This resonance can be utilized to create a cloak of invisibility about ocean objects against incident surface waves. The invisibility cloak of water waves must detour wave rays about the object as if the object does not exist. Incident waves, as a result, must be able to propagate forward without interruption, i.e., with no trace of diffraction.

Specifically, consider a monochromatic surface wave train with wavelength $\lambda_s = 2\pi/k_s$ arriving from $x = -\infty$. Our objective is to create a cloaked buffer zone about $x = 0$ where our hypothetical floating object resides. We will show that a series of properly architected bottom undulations can effectively transfer the energy from the incident surface wave to internal waves, i.e., from the surface to within the body of water, and vice versa. Internal waves can later be fully recovered back to the surface at downstream. These recovered surface waves in the downstream carry no trace of the object because they have bypassed the encounter via nonlinear interaction with our bottom-mounted cloak; hence, invisibility is achieved.

In contrast to electromagnetic and acoustic cloaking based on coordinate transformation [6] and the use of metamaterials [7–12], where so far the invisibility is limited to a single frequency (radar and microwave), and also perfect invisibility is impossible [8,13], we prove theoretically that in our scheme a complete cloaking is achievable. We also present computational evidence of monochromatic and broadband cloaking. We note that, specific to ocean applications, the cloaking is more important in *protecting* ocean objects against powerful incoming waves than making their trace invisible.

Consider a two-layer density stratified fluid with ρ_u, ρ_ℓ and h_u, h_ℓ, respectively, upper and lower layer densities and depths (Fig. 1). In each layer, we assume that the fluid is homogeneous, incompressible, immiscible and inviscid, and we neglect the effects of surface tension. Under these assumptions a two-layer fluid admits two types of propagating waves associated with a given frequency ω (see Supplemental Material SI for the governing equation [14]): a surface wave with the wave number k_s and an interfacial wave with the wave number $k_i \gg k_s$, where k_s, k_i are solutions of the so-called dispersion relation

$$\begin{aligned}\mathcal{D}(k,\omega) \equiv\ & \omega^4(\mathcal{R} + \coth kh_u \coth kh_\ell) \\ & - \omega^2 gk(\coth kh_u + \coth kh_\ell) \\ & + g^2k^2(1-\mathcal{R}) = 0, \end{aligned} \tag{1}$$

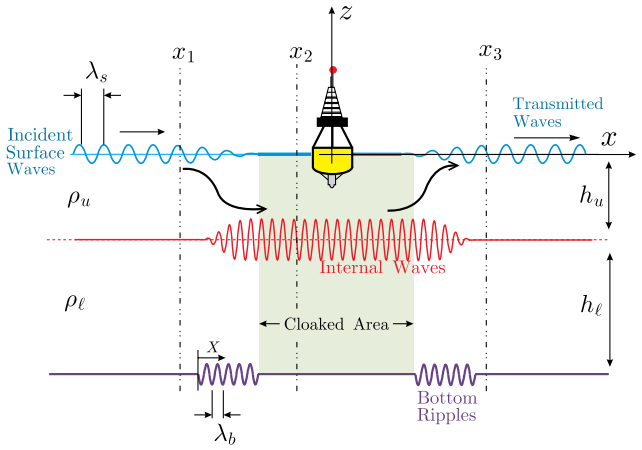

FIG. 1 (color online). Schematic representation of cloaking mechanism in a two-layer density stratified fluid. An incident wave of wave number $k_s = 2\pi/\lambda_s$ gives its energy to an interfacial wave k_i, of the same frequency, over a patch of bottom ripples $k_b = k_i - k_s$ hence leaving a cloaked buffer zone of invisibility. The interfacial wave can be recovered at the downstream ($x > 0$) by the same mechanism.

in which $\mathcal{R} = \rho_u/\rho_\ell$ is the density ratio and g is gravity acceleration.

Bottom roughnesses scatter both surface and interfacial waves (e.g., [15]). If bottom irregularities follow a specific pattern then scattered waves may constructively interfere to form one single ray with a specific wavelength. This phenomenon is called Bragg resonance of water waves named after its close cousin phenomenon in solid state physics of crystals [16]. Contrary to Bragg reflection from crystals which is a linear phenomenon, Bragg resonance of water waves is a nonlinear phenomenon. In perturbation expansion of governing equations in terms of a small parameter (usually wave steepness ka, k being the wave number and a the amplitude of wave) Bragg resonance occurs at the second order (class I), third order (class II and III), and higher orders of nonlinearities [17,18].

In a homogeneous fluid if bottom has periodic undulations with the wavelength equal to half of the wavelength of the incident wave, then incident waves will be (partially) reflected [17–21]. The reflection coefficient (ratio of amplitude of reflected wave to the amplitude of incident wave) is a function of length of the patch of undulations and asymptotically approaches one as the extent of the patch stretches to infinity.

For a two-layer density stratified fluid we have recently shown [22,23] that at the leading (second) order nonlinearity six scenarios of Bragg resonance is possible. If we have an incident surface wave (k_s), then depending on bottom properties the resonant wave may be a reflected surface wave, a reflected interfacial wave or a transmitted interfacial wave. If the incident wave is an interfacial wave, then the resonant wave may be a reflected interfacial wave, a reflected surface wave or a transmitted surface wave.

For cloaking purposes we are interested in cases where the resonant wave is a transmitted wave. Specifically, consider an incident surface wave of wave number k_s. Now, if bottom undulations wave number k_b satisfies the resonance condition $k_b = k_i - k_s$, then over the patch of bottom ripples the surface wave gives its energy to the interfacial wave (see left side of Fig. 1). If amplitude of incident surface wave and resonant interfacial wave is given, respectively, by $A_s(X)$ and $A_i(X)$ where X is horizontal dimension measured from the beginning of the ripple patch, then using multiple scales techniques it can be shown that [22]:

$$A_s(X) = \alpha \cos(\kappa X), \qquad A_i(X) = \beta \sin(\kappa X), \tag{2}$$

where α, β and κ are functions of ocean parameters (see Supplemental Material SII [14] for expressions of these coefficients). If the length of the bottom patch is exactly $X_b = \pi/(2\kappa)$ then Eq. (2) predicts that the amplitude of incident wave reaches exactly zero at the end of the patch. Physically speaking, at this distance surface wave energy has been completely transferred to the interface. The same bottom patch can in reverse transfer the energy of an incident interfacial wave to a resonant surface wave and is used on the right hand side of the ocean object to recover the surface wave (Fig. 1). Therefore, theoretically, a perfect cloaking is achieved.

If the incident wave train is polychromatic, i.e., with many components forming a spectrum of waves, leading order cloaking is achieved by the superposition of proper bottom undulations for each of incident wave components. This, usually, does not require additional space, but just a polychromatic bottom undulations, hence can be readily achieved.

Theoretical analysis of broadband cloaking is, however, very limited. Usually when more than just a few wave components interact simultaneously it is algebraically tedious—if not impossible—to track their interactions. This fact becomes more highlighted when we notice that for an accurate prediction of the evolution of a spectrum of waves over a patch of bottom ripples several nonlinear interaction scenarios including, but not limited to, sub and superharmonic generations [24,25], triad and quartet resonance between waves [26–28] and high-order Bragg resonances [22,23] must be taken into account. To address the problem of many (typically $N = O(10^4)$] waves interacting and to consider an arbitrary order of nonlinearity [typically $M = O(10)$ in terms of perturbation expansion) we have recently extended a direct simulation scheme based on a high-order spectral method (HOS), originally derived to study nonlinear wave-wave [29] and wave-bottom [17] interactions, to a two-layer density stratified fluid with finite-depth upper and lower layers ([22], where extensive convergence tests and validations with experimental data are also provided). Here we use HOS to, besides validating our

theoretical predictions, study the initial-value problem of surface waves (monochromatic and broadband) impinging upon our cloak of invisibility.

We first consider a monocrhomatic incident surface wave of wave number and frequency $k_sH = 0.34$ and $\omega\sqrt{H/g} = 0.36$, with $H = h_u + h_\ell$, in a two-layer density stratified fluid of $\mathcal{R} = 0.95$ and $h_u/H = 1/2$ (relevance of chosen values to real life applications are discussed in the Supplemental Material, SIII). At $t/T = 0$ it is assumed that the water surface is calm and a train of waves arrives from $x = -\infty$ to the domain of our interest $-70 < k_sx < 70$. A bottom patch of dimensionless wave number $k_bH = k_iH - k_sH = 4.86$ (where k_i is the interfacial wave solution of (1) for frequency ω) forms a resonance between k_s, k_i. From multiple scales analysis results (2) it is seen that if $n_b = k_b/(4\kappa)$ number of bottom undulations are placed on the seafloor all the energy of k_s is transformed to k_i. Comparison of theoretical results (2) (dashed lines) with direct simulation of initial-value problem of this example after a steady state is reached (solid lines) are presented in Fig. 2. For direct simulation we have chosen $N = 2048$, $M = 3$, $T/\delta t = 64$ for which the computation is converged. Figure 2 shows a good agreement between analytical results and direct computations. The cloaked zone is clearly formed in the area of $-6 < k_sx < 6$ where surface activity is minimal.

To better assess the transient response of our cloak as it encounters the incident wave and until it reaches a steady state, Fig. 3 shows the amplitude of waves predicted by solving the initial-value problem using our spectral-based direct simulation scheme. Amplitude of surface waves at three stations of x_1, x_2, and x_3 (cf. Fig. 1), respectively, upstream, in the cloaked zone and downstream, are plotted in Figs. 3(a)–3(c). In each figure the amplitude of waves in the presence and in the absence of the cloak is presented. In upstream [Fig. 3(a)] and in the absence of the cloak the monochromatic wave train marches forward without any interruption; hence, no variation in the amplitude is expected. If the cloak exists Fig. 3(a) shows again no variation in the upstream amplitude which implies that the cloak does not reflect any waves. In the cloaked zone however, the surface amplitude is greatly reduced [Fig. 3(b)]. The observed nonzero surface activity (i.e., the error) is mainly due to the image of the interfacial waves on the surface. Because of its short wavelength this image is easily detectable in Fig. 2 on the surface of water in the cloaked zone. Note that these short waves are not seen outside the cloak where interfacial wave amplitude is small. Finally, Fig. 3(c) shows the downstream spectrum. With the cloak and after a transition period is passed, the downstream spectrum approaches that of the upstream. The three Figs. 3(a)–3(c) show the performance of our bottom-mounted cloak in creating a buffer zone of

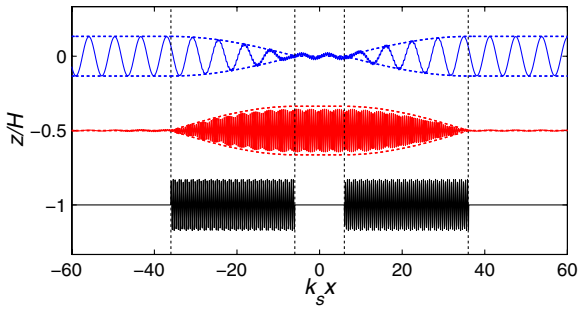

FIG. 2 (color online). Cloaking against a monochromatic incident surface wave. Plotted results are analytical solution based on multiple scales theory (2) (dashed line), and direct simulation of HOS (solid line). A surface wave $k_sH = 0.34$ enters from $x = -\infty$ and exchanges its energy to the interface as it travels over the first bottom patch ($-36 < k_sx < -6$). In a reverse process the interfacial wave gives back its energy to the surface as it travels over the second patch of bottom ripples ($6 < k_sx < 36$). As a result, a cloaked buffer zone ($-6 < k_sx < 6$) is formed where surface activity is very small. Surface and interfacial elevations are magnified by factors of, respectively, 1000 and 50 for easier realization.

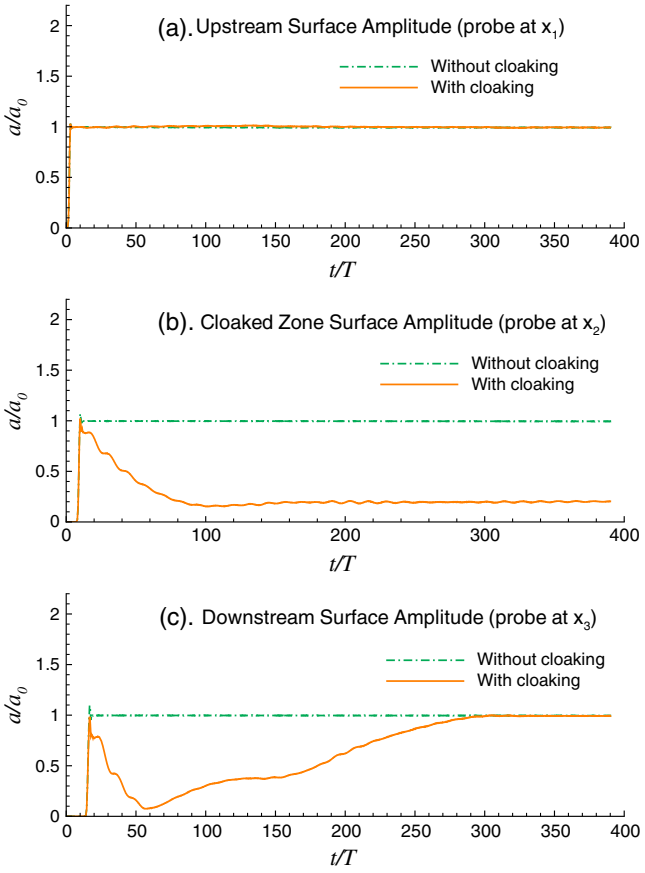

FIG. 3 (color online). Time history of evolution of surface wave amplitude obtained from direct simulation at (a) $k_sx_1 = -40$, (b) $k_sx_2 = 0$, and (c) $k_sx_3 = 40$ (cf. Fig. 1). Results plotted are the upstream (incident) wave in the absence of bottom undulations given for the reference (dash-dotted line), and the surface wave amplitude in the presence of cloaking (solid line).

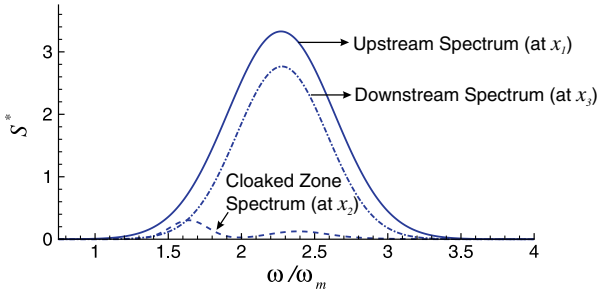

FIG. 4 (color online). Cloaking against a spectrum of waves. Plotted curves are the upstream (incident) wave spectrum (solid line), downstream spectrum (dash-dotted line), and spectrum in the cloaked zone (dashed line). $\int S^* d\omega = \sum_{i=1,5} 1/2(a_i/a_m)^2$, with a_i amplitude of each individual wave normalized by a_m the amplitude of the median wave.

invisibility, and also in recovering the wave to the surface with the minimal loss.

For a broadband spectrum of incident waves, leading order cloaking is achieved by the superposition of bottom profiles required by each of wave components in the spectrum. Consider a broadband Gaussian spectrum of incident waves (Fig. 4, solid line) arriving to the location of our hypothetical floating object to be cloaked. For direct simulation purposes, we discretize this spectrum into five individual waves and superimpose the five bottom wave number on top of each other to form a polychromatic patch of corrugations (details of numerical simulation is provided in the Supplemental Material SIV [14]). Figure 4 presents the result of direct simulation of an incident broadband spectrum as it travels over the bottom cloak. After a steady state is reached the cloaked zone (dash line) experiences negligible wave activity, only $\sim$%5 of incident wave energy. The downstream spectrum (dash-dotted) is close to the incident spectrum recovering more than %70 of incident wave energy. Besides the source of error already discussed for monochromatic cloaking, in the case of a broadband spectrum nonlinear interactions between waves within the spectrum are also affecting the performance of the cloaking. A smart design of an efficient (higher-order) broadband cloak requires care to avoid unwanted resonances.

Results obtained here are also valid in the presence of a floating object. An example of cloaking in the presence of a heaving disturbance is discussed in the Supplemental Material SV [14]. If the bottom is not flat (e.g., sloped) then ripples can be adjusted in order to retain the high performance of the cloaking scheme (see Supplemental Material SVI [14]). It is to be noted that the demonstrated scheme for unidirectional cloaking can be extended to omnidirectional cloaking by the use of radial Bragg resonance (i.e., concentric circular bottom undulations). Nevertheless, in the context of ocean waves, due to the refraction of waves in (relatively) shallower waters, this is of less importance and hence is not pursued here.

In summary, we have demonstrated that floating objects in stratified fluids can be cloaked against broadband incident waves by properly architecting the bottom corrugations. The concept behind the presented scheme is based on nonlinear resonance of surface and interfacial waves with the bottom topography and is obtained due to the dispersive nature of gravity waves. Perfect cloaking against monochromatic waves can theoretically be achieved and was further investigated via a direct high-order spectral scheme. Broadband cloaking was also elucidated and its performance is discussed. The cloak introduced here is the alignment of bottom corrugations only, and therefore is surface noninvasive. Cloaking in seas by bottom modifications may play a role in protecting near shore or offshore structures (buoys) and in creating shelter for fishermen during storms. In reverse it can result in disappearance and appearance of surface waves in areas where sandbars (or any other appreciable bottom variations) exist.

Bragg scattering or resonance, although may differ in details, but is a common concept in solid state physics [30,31], optics (e.g., [32]), acoustics (e.g., [33]) and hydrodynamics [17–19]. The idea demonstrated here may have similar implications in any system admitting Bragg resonance and if its medium can be freely architected.

I would like to thank Dr. Y. Liu and Dr. R. Karimi for careful reading of the manuscript and valuable comments. The support from the American Bureau of Shipping is greatly acknowledged.

[1] C. Garrett and W. Munk, Annu. Rev. Fluid Mech. **11**, 339 (1979).
[2] D. Sigman, S. Jaccard, and G. Haug, Nature (London) **428**, 59 (2004).
[3] J. T. Holt and S. A. Thorpe, Deep-Sea Research, Part I **44**, 2087 (1997).
[4] W. Choi and R. Camassa, Phys. Rev. Lett. **77**, 1759 (1996).
[5] L. Boegman, J. Imberger, G. N. Ivey, J. P. Antenucci, and A. Hogg, Limnol. Oceanogr. **48**, 895 (2003).
[6] A. Ward and J. Pendry, J. Mod. Opt. **43**, 773 (1996).
[7] J. B. Pendry, D. Schurig, and D. R. Smith, Science **312**, 1780 (2006).
[8] U. Leonhardt, Science **312**, 1777 (2006).
[9] S. a. Cummer, B.-I. Popa, D. Schurig, and D. R. Smith, Phys. Rev. E **74**, 1 (2006).
[10] D. Schurig, J. J. Mock, B. J. Justice, S. A. Cummer, J. B. Pendry, A. F. Starr, and D. R. Smith, Science **314**, 977 (2006).
[11] Y. Urzhumov and D. Smith, Phys. Rev. Lett. **107**, 074501 (2011).
[12] M. Farhat, S. Enoch, S. Guenneau, and a. Movchan, Phys. Rev. Lett. **101**, 134501 (2008).
[13] P. Yao, Z. Liang, and X. Jiang, Appl. Phys. Lett. **92**, 031111 (2008).
[14] See Supplemental Material at http://link.aps.org/supplemental/10.1103/PhysRevLett.108.084502 for details of governing equations, explicit forms of coefficients

presented in the main text, discussion on the relevance to the real world applications, and two illustrative examples that supplement the main text.

[15] M.-R. Alam and C. C. Mei, J. Fluid Mech. **587**, 73 (2007).
[16] W. H. Bragg and W. L. Bragg, Proc. R. Soc. A **88**, 428 (1913).
[17] Y. Liu and D. K.-P. P. Yue, J. Fluid Mech. **356**, 297 (1998).
[18] M.-R. Alam, Y. Liu, and D. K. P. Yue, J. Fluid Mech. **643**, 437 (2010).
[19] C. C. Mei, J. Fluid Mech. **152**, 315 (1985).
[20] A. Davies, Dynamics of Atmospheres and Oceans **6**, 207 (1982).
[21] X. Hu and C. Chan, Phys. Rev. Lett. **95**, 154501 (2005).
[22] M.-R. Alam, Y. Liu, and D. K. P. Yue, J. Fluid Mech. **624**, 191 (2009).
[23] M.-R. Alam, Y. Liu, and D. K. P. Yue, J. Fluid Mech. **624**, 225 (2009).
[24] P. J. Bryant, J. Fluid Mech. **59**, 625 (1973).
[25] C. Mei and U. Unluata, in *Waves on Beaches and Resulting Sediment Transport* (Academic Press, New York, NY, 1971), p. 181.
[26] F. K. Ball, J. Fluid Mech. **19**, 465 (1964).
[27] F. Wen, Phys. Fluids **7**, 1915 (1995).
[28] M.-R. Alam, J. Fluid Mech. **691**, 267 (2012).
[29] D. G. Dommermuth and D. K. P. Yue, J. Fluid Mech. **184**, 267 (1987).
[30] P. J. Martin, B. G. Oldaker, A. H. Miklich, and D. E. Pritchard, Phys. Rev. Lett. **60**, 515 (1988).
[31] E. Fermi and L. Marshall, Phys. Rev. **71**, 666 (1947).
[32] G. Kryuchkyan and K. Hatsagortsyan, Phys. Rev. Lett. **107**, 053604 (2011).
[33] L. Feng, X.-P. Liu, M.-H. Lu, Y.-B. Chen, Y.-F. Chen, Y.-W. Mao, J. Zi, Y.-Y. Zhu, S.-N. Zhu, and N.-B. Ming, Phys. Rev. Lett. **96**, 014301 (2006).

Broadband cloaking in Stratified Seas
Supplementary Notes

Mohammad-Reza Alam[1]
[1]*Department of Mechanical Engineering, University of California, Berkeley, CA 94720, USA*

I. GOVERNING EQUATIONS FOR A TWO-LAYER DENSITY STRATIFIED FLUID

We define a Cartesian coordinate system with the x-axis on the mean free surface and the z-axis positive upward. Based on assumption stated in the main text the fluid motion in each layer is irrotational and can described by the velocity potential $\phi_u(x,z,t)$ or $\phi_\ell(x,z,t)$. Fully nonlinear governing equations are [1–4]:

$$\nabla^2\phi_u = 0 \qquad -h_u+\eta_\ell < z < \eta_u \tag{.1a}$$
$$\nabla^2\phi_\ell = 0 \qquad -h_u-h_\ell+\eta_b < z < -h_u+\eta_\ell \tag{.1b}$$
$$\eta_{u,t}+\eta_{u,x}\phi_{u,x}-\phi_{u,z}=0 \qquad z=\eta_u \tag{.1c}$$
$$\phi_{u,t}+\tfrac{1}{2}(\phi_{u,x}^2+\phi_{u,z}^2)+g\eta_u=0 \qquad z=\eta_u \tag{.1d}$$
$$\eta_{\ell,t}+\eta_{\ell,x}\phi_{u,x}-\phi_{u,z}=0 \qquad z=-h_u+\eta_\ell \tag{.1e}$$
$$\eta_{\ell,t}+\eta_{\ell,x}\phi_{\ell,x}-\phi_{\ell,z}=0 \qquad z=-h_u+\eta_\ell \tag{.1f}$$
$$\rho_u[\phi_{u,t}+\tfrac{1}{2}(\phi_{u,x}^2+\phi_{u,z}^2)+g\eta_\ell]- \rho_\ell[\phi_{\ell,t}+\tfrac{1}{2}(\phi_{\ell,x}^2+\phi_{\ell,z}^2)+g\eta_\ell]=0 \qquad z=-h_u+\eta_\ell \tag{.1g}$$
$$\eta_{b,x}\phi_{\ell,x}-\phi_{\ell,z}=0 \qquad z=-h_u-h_\ell+\eta_b. \tag{.1h}$$

where η_u=$\eta_u(x,t)$, η_ℓ=$\eta_\ell(x,t)$, are respectively the free surface and interface wave elevations. Equations (.1a) and (.1b) are continuity equations for respectively upper and layer fluids; equations (.1c), (.1e), (.1f) and (.1h) are kinematic boundary conditions for respectively surface, the upper layer of the interface, the lower layer of the interface and the bottom. Kinematic boundary condition (.1c) guarantees that a fluid particle at the surface of the upper layer fluid never leaves the surface of the upper layer fluid. Kinematic boundary conditions on the interface, i.e. (.1e) and (.1f), guarantee that fluid particles of upper and lower layer fluid never intrude the other, and kinematic boundary condition on the bottom (.1h) guarantees that a fluid particle at the bottom never leaves the bottom. Two dynamic boundary conditions (.1d) and (.1g) satisfy the continuity of pressure at the free surface and the interface. If governing equations (.1) are linearized and a progressive wave solution, i.e. in the form $f(kx-\omega t)$, is sought it turns out that f has the form of a sinusoidal wave and that the wavenumber and frequency for such a solution must satisfy the dispersion relation

$$\mathcal{D}(k,\omega)\equiv\omega^4(\mathcal{R}+\coth kh_u\coth kh_\ell)-\omega^2gk(\coth kh_u+\coth kh_\ell)+g^2k^2(1-\mathcal{R})=0. \tag{.2}$$

It is easy to see that for a given wavenumber $k>0$, (.2) has four solutions: $\pm\omega_s(k),\pm\omega_i(k)$, with $\omega_s>\omega_i>0$, where $\pm\omega_s(k)$ and $\pm\omega_i(k)$ are denoted as the surface-mode and interfacial-mode waves respectively [3].

II. COEFFICIENTS OF EQUATION .2 [3]

If we take α as the amplitude of the incident wave, then

$$\beta=-\frac{\kappa C_g^r}{\mathcal{N}}\alpha \tag{.3}$$

where $\kappa^2\equiv-\mathcal{M}\mathcal{N}/(C_gC_g^r)$, $C_g=\mathrm{d}\omega/\mathrm{d}k$ and $C_g^r=\mathrm{d}\omega/\mathrm{d}k^r$ are group velocity of the incident and the resonance generated wave (k and ω are the wavenumber and frequency of incident wave and k^r is the wavenumber of the resonance generated wave). Other coefficients are

$$\begin{aligned}\mathcal{M}=\quad&\omega^3d\lambda\lambda^rk\sinh kh_\ell/(2\mathcal{R}gk\sinh kh_\ell-3\mathcal{R}\lambda gk\sinh kh_\ell\ \cosh kh_u+3\mathcal{R}\lambda\omega^2\sinh kh_\ell\ \sinh kh_u\\&+\mathcal{R}g\lambda^2k\sinh kh_\ell+3\omega^2\lambda^2\cosh kh_\ell-g\lambda^2k\sinh kh_\ell)/(2\sinh kh_\ell\ \sinh k^rh_\ell)\end{aligned}$$

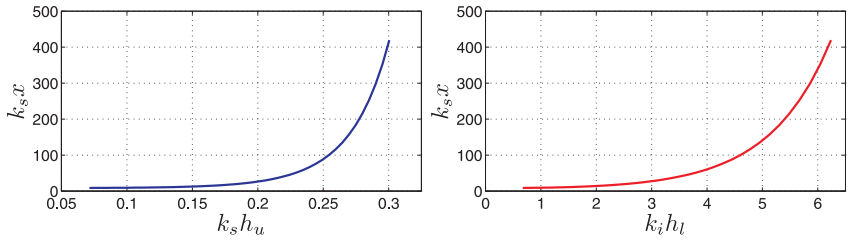

FIG. 1: The distance required for a perfect cloaking ($k_s x$) as a function of shallownesses of surface and interfacial waves ($k_s h_u, k_i h_\ell$). Parameters are the same as in figure 2 of the main text ($h_u/H = 1/2, \mathcal{R} = 0.95$). The required distance of rippled bottom for a perfect cloaking increases exponentially fast with the increase in the water depth. This increase can be partially compensated by increasing the amplitude of bottom undulations.

$$\begin{aligned}\mathcal{N} = \quad & \omega^3 d\lambda\lambda^r k^r \sinh k^r h_\ell/(2\mathcal{R}gk^r \sinh k^r h_\ell - 3\mathcal{R}\lambda^r gk^r \sinh k^r h_\ell \ \cosh k^r h_u \\ & +3\mathcal{R}\lambda^r\omega^2 \sinh k^r h_\ell \ \sinh k^r h_u + \mathcal{R}g\lambda^{r2}k^r \sinh k^r h_\ell + 3\omega^2\lambda^{r2}\cosh k^r h_\ell \\ & -g\lambda^{r2}k^r \sinh k^r h_\ell)/(2\sinh kh_\ell \ \sinh k^r h_\ell)\end{aligned}$$

with $\lambda = \cosh(kh_u) - (gk/\omega^2)\sinh(kh_u)$, $\lambda^r = \cosh(k^r h_u) - (gk^r/\omega^2)\sinh(k^r h_u)$, and d is the amplitude of bottom undulations.

III COMMENT ON RELEVANCE TO PRACTICAL APPLICATIONS

The science and technology of cloaking is at its early stage of development and far from real application [5–8]. Nevertheless chosen values for examples presented here are not unrealistic for ocean scenarios. Examples and parameter values similar to what was presented here, although may not be very typical and ubiquitous, but may be realized in the real scenarios.

In real ocean the dimensionless depth of the thermocline h_u/H can vary from zero, when the water is almost homogeneous and the surface is starting to heat up, to almost one. The latter is specifically realized near the continental slopes when the deep ocean thermocline encounters the shelf. For both monochromatic and spectrum cloaking we have chosen h_u/H=1/2. The density ratio $\mathcal{R}$ in the ocean is typically weak ($\mathcal{R}$ >0.95). While our theory and numerical scheme is valid for any density ratio, with the hope of easing the path for experimental investigation of presented mechanism, we have chosen $\mathcal{R}$=0.95 which is typically considered a strong stratification. For a water of total depth 8m, the monochromatic surface wave considered here has the wavelength of $\sim$ 110 m. For this set of chosen parameters the needed bottom patch is $\sim$ 700m. Note that the cloaked area can be as long as required, hence one bottom patch can be used to protect the surface of the entire field, say an offshore wind farm.

It is to be Noted that at the depth of $\sim$ 8 meters (given as an example above), offshore structures are rarely floating and are more likely bottom mounted. The submerged part of the structure therefore goes beneath the thermocline and may be vulnerable to the action of interfacial waves. More generally, all offshore floating structures are connected to the seabed either by mooring lines (that can be slack or tight) or by the structure itself that goes to the bottom. Vulnerability of the bottom-connector against strong interfacial waves, the current they generate, and their (potentially) breaking has to be carefully investigated before any plan for implementation of the presented idea.

We further note that the group velocity of interfacial wave is typically much smaller that the group velocity of surface waves. As a result and upon occurrence of the resonance discussed here, generated interfacial waves will have very high amplitudes and steepnesses, hence inducing strong oscillatory currents near the thermocline and even beyond. This may pose an additional danger to the parts of the structure/buoy which are close to the thermocline.

Theoretical efficiency of presented mechanism is unity for any shallownesses of upper/lower layer and surface/interfacial waves. In other words there is no theoretical requirement on the values or the order of magnitudes of $k_s h_u, k_s h_\ell, k_i h_u$ and $k_i h_\ell$. However, from engineering point of view and for the purpose of practical implementation, it is necessary that none of the shallownesses exceed the order of unity. This is because the number of required bottom ripples increases exponentially as the water depth increases (see figure 1). Engineering constraints may therefore pose a limitation on the maximum depth for which this idea is applicable in the real ocean.

Nevertheless, specific examples with non-unrealistic parameters can be presented for which shallownesses are orders of magnitude different from each other. For instance, consider a two-layered stratified sea of R=0.95 and h_u/H=0.9 (i.e. thermocline close to the bottom). For this hypothetical example, $k_i h_u = O(100)$ while $k_s h_u = O(1)$ and

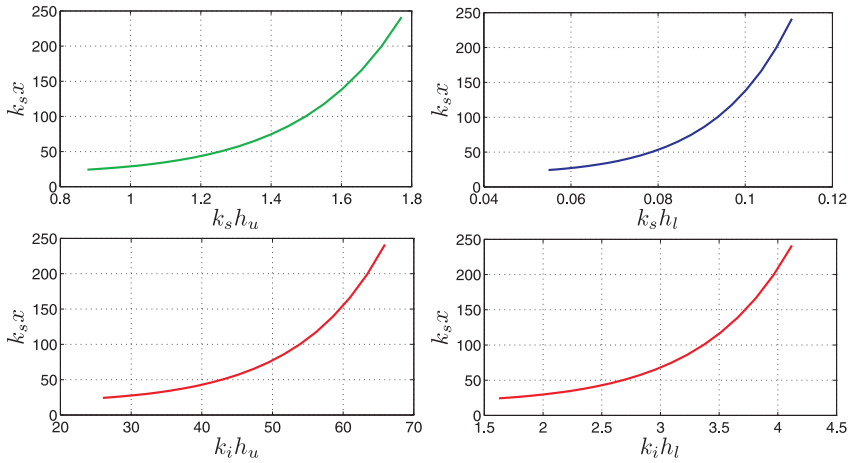

FIG. 2: The distance required for a perfect cloaking ($k_s x$) as a function of shallownesses of surface and interfacial waves ($k_s h_u, k_s h_\ell, k_i h_u, k_i h_\ell$). Parameters are $h_u/H = 0.94$, $\mathcal{R} = 0.95$, and for $k_s h_u$=1.17, $\omega\sqrt{H/g}$=1. Note that the interfacial wave is (nearly) a short wave with respect to either the upper and lower layer.

$k_s h_\ell = O(0.1)$ and a perfect cloaking is achieved within a distance of $\sim O(10)$ times the wavelength of the incident wave (figure 2- note that $k_s x = 2\pi x/\lambda_s$). The case of $k_s h_u$=1.1 of this example is correspond to, for instance, a surface wave of wavelength λ_s=100 meters traveling in a two-layer fluid of total depth H=20 meters. The distance required to transfer the entire energy to the interfacial waves is $x \sim 600$ meters. The resonant interfacial waves however are very short $\lambda_i \sim 2$m.

IV. DETAILS OF NUMERICAL SIMULATION OF A BROADBAND SPECTRUM

Here we present details of numerical simulation of a Gaussian incident wave spectrum (fig. 4, Solid line) as it travels over a patch of bottom topography. The bottom is particularly designed to cloak a buffer zone (c.f. fig. 1). Note that the major part of the energy of the typical ocean wave spectrum (wind waves) are in the frequency range of typically $0.05 - 0.3$ Hz [9] and therefore the chosen spectrum of fig. 4 of the main text is not unrealistic.

For numerical simulation using our pseudo-spectral method of HOS we need to break the spectrum of fig. 4 of the main text into individual waves. To do so, we balance the total energy by dividing the spectrum into five waves of respectively $k_s H$ =0.165, 0.210, 0.255, 0.300, 0.345 with respective amplitudes a/a_m=0.41, 0.80, 1.00, 0.80, 0.41, where a_m/H=3.4e-5 is the normalized amplitude of median wave. Five bottom components correspond to each of these waves are then superimposed on the bottom patch with each has an amplitude of d/H=0.1. A random phase is added to each phase. Direct simulation parameters are $N = 2048$, $M = 3$, $T/\delta t$=64 and the results are verified to be converged for these parameters.

V. CLOAKING IN THE PRESENCE OF A REACTING DISTURBANCE

Here we study the performance of our cloaking scheme in the presence of a heaving disturbance whose amplitude is a function of amplitude of waves that it encounters. Such a disturbance approximates the effect of a heavy (i.e. oscillating vertically) floating object, e.g. an actively stabilized offshore platform. To achieve this, we apply a localized Gaussian pressure distribution at $x = 0$ (normalized full width at half maximum $k_s \times$ fwhm=0.935) whose strength is proportional to the water surface elevation at $x = 0$ with a phase lag of $\delta\psi/T$=0.3.

Simulation parameters and initial condition are the same as those chosen for figs 2 & 3 in the main text. Fig. 3 shows the surface and interfacial waves in the presence of the disturbance. Compare to fig. 2 of the main text, the amplitude of surface activity at the cloaked zone has increases, but still is much less that that amplitude of the incident wave. Note that because the cloaked area receives almost no surface wave the presence of the disturbance (only considered in the direct simulation) has almost no effect on the upstream/downstream propagating waves.

The performance of our cloaking is more highlighted in fig. 4 where the surface elevation in upstream, downstream and in the middle zone is compared in the presence and absence of the cloaking. In fig. 4a, where the surface wave

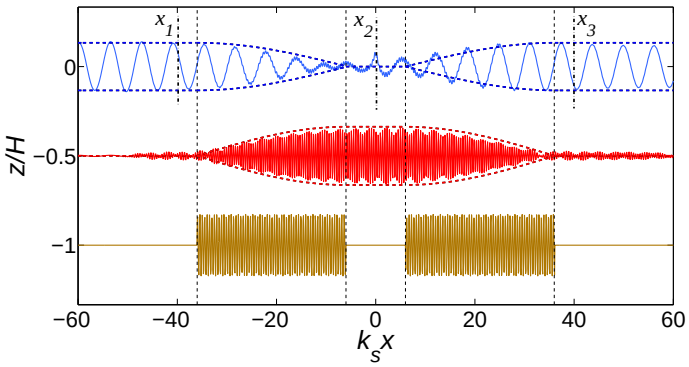

FIG. 3: Cloaking against a monochromatic incident surface wave. Plotted results are analytical solution based on multiple scales theory (.2 of the main text) (- - -), and direct simulation of HOS (——). In the latter, the effect of a floating object is simulated by a narrow-band pressure distribution whose amplitude varies with the surface elevation at $x = 0$ and acts near the origin with a Gaussian distribution with $k_s \times$ fwhm=0.935[a]. A surface wave $k_s H$ =0.34 enters from $x = -\infty$ and exchanges its energy to the interface as it travels over the first bottom patch ($-36 < k_s x < -6$). In a reverse process the interfacial wave gives back its energy to the surface as it travels over the second patch of bottom ripples ($6 < k_s x < 36$). As a result, a cloaked buffer zone ($-6 < x < 6$) is formed where surface activity is very small. Surface and interfacial elevations are magnified by factors of respectively 1000 & 50 for easier realization.

[a]fwhm=Full width at half maximum, is the width of a Gaussian curve at a height (i.e. the vertical coordinate) equal to half of the peak height. For a normal distribution: $f(x) = 1/(\sigma\sqrt{2\pi})\exp[-(x-x_0)^2/(2\sigma^2)]$, then fwhm=$2\sigma\sqrt{2\ln 2}$.

amplitude at x_1 (c.f. fig. 1) is plotted, the incident wave amplitude (dashed line) in the absence of both the bottom and the floating object is obviously constant and is given to serve as a reference. If bottom patch does not exist the incident wave excites the floating object and generates waves that travel both upstream and downstream (dash-dot lines). However, if cloak of bottom ripples present (solid line) after a transition period the upstream (fig. 4a for a probe at x_1) and downstream (fig. 4c for a probe at x_3) amplitudes approach that of the incident wave (dashed line). Amplitude of surface elevation at x_2 is shown in fig. 4b and the effect of cloaking is clear from small amplitude of water surface at that point.

Effect of our proposed cloaking against a broadband wave with the same disturbance is also studied. Figure 5 presents the result of direct simulation with and without the bottom cloak. With the bottom cloak and after a steady state is reached the downstream spectrum (dash-dot) is very close to the incident spectrum (solid-line). The performance of superimposed cloaking is appreciated when this is compared with the downstream spectrum in the absence of cloaking (dash-double dots). Fig. 5 also shows that the oscillation of the floating object is significantly reduced if cloaking is applied.

VI. CLOAKING OVER A SLOPED BOTTOM

Over the continental shelf the bottom is typically mildly sloped. Over a slope and as the water depth changes waves deform and the condition for the Bragg resonance is modified. The change in the wave characteristics due to the sole effect of the bottom slope is called wave shoaling and has been extensively studied for homogeneous as well as stratified waters [e.g. 10, 11]. The Bragg resonance condition in the presence of bottom variations can be addressed using regular perturbation techniques [e.g. 12] or mild-slope equations and its variations [e.g. 13, 14]. On a weakly sloped bottom Bragg condition slowly changes as the water depth changes. The change is due to the shoaling of the incident/interacting waves and also due to the effect of water shallowness on the strength of the resonance.

For a high-performance cloaking the effect of sloped bottom on the resonance condition needs to be carefully addressed. If water depth changes then the wavenumber of bottom ripples k_b, the number of ripples n_b required to achieve a perfect transfer of energy, and the amplitude of ripples a_b may need to change. The latter two parameters appear as a multiplication (i.e. $n_b \times a_b$) in the Bragg resonance formula and therefor leave a degree of freedom in choosing their values. Here we assume that a_b is given and constant and only consider the variation of n_b.

Let assume h_u is constant and h_ℓ varies. Physically this scenario is associated with a constant depth thermocline with a sloped topography (c.f. fig. 7). The wavenumber of bottom ripples k_b- required to satisfy the Bragg resonance condition- is a weak function of the bottom variations as is seen in fig. 6.a. The number of bottom undulations n_b,

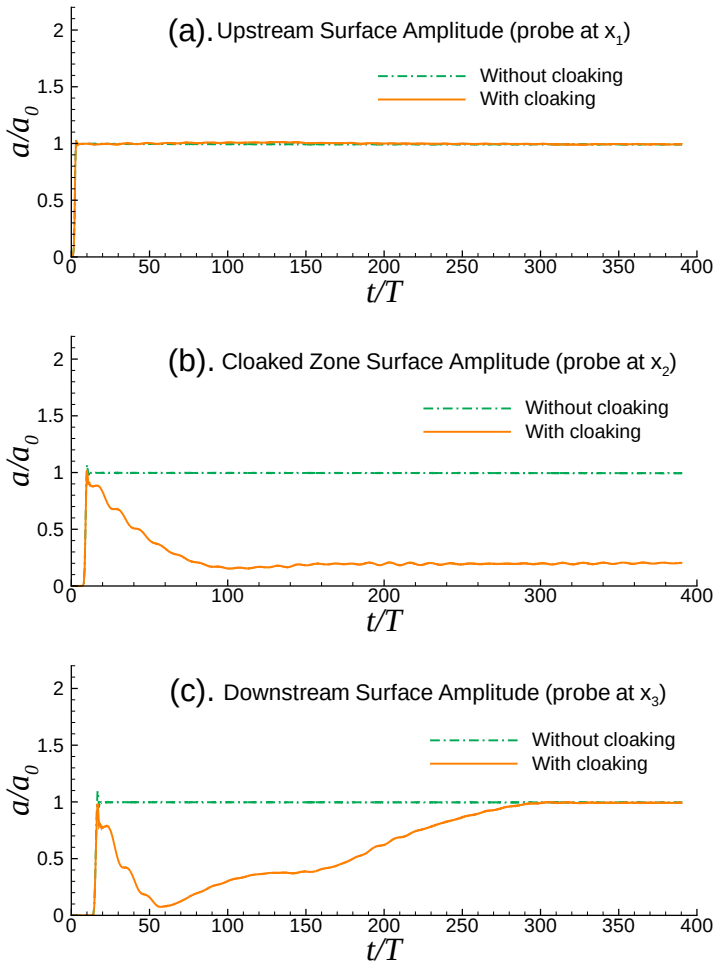

FIG. 4: Time history of evolution of surface wave amplitude obtained from direct simulation at a) $k_s x_1$=-40, b) $k_s x_2$=0, and c) $k_s x_3$=40 (c.f. Fig. 1 of the main text). Results plotted are the upstream amplitude of the surface wave in the absence of the floating object and bottom undulations given for the reference (- - -), the amplitude of surface wave in the presence of effect of object, but with no cloaking (– · –), and the amplitude of the surface wave with object and cloaking (——). If the object is not cloaked diffracted and radiated waves affect both upstream and downstream elevation. In the presence of cloaking, object amplitude is greatly reduced (b) and once steady state is achieved its trace is disappeared from the upstream and downstream

however, changes considerably with the change in the lower layer depth (h_ℓ). As h_ℓ increases the distance between the interface and the bottom increases and therefore more ripples will be required to transfer the same amount of energy from the surface to the interface and vice versa. Note that the increase in the frequency of the incident wave ($\omega\sqrt{h/g}$) has a similar effect on n_b.

The direct scheme of high-order spectral scheme discussed in the main text has been recently extended to take into account the effect of the bottom slope. Here we use HOS to demonstrate the robustness of our cloaking scheme against a mild slope bottom variations and discuss techniques to improve results. Specifically, figure 7.a presents result of the direct simulation of cloaking against a monochromatic incident surface wave over a sloped bottom. The assumptions are the same as in fig. 2 of the main text, except a uniform sloping bottom ($-50 < k_s x < 50$) that reduces the h_ℓ by %20 (marked by short vertical bars on the bottom). In fig. 7.a the bottom is assume to have the same k_b and n_b as the flat bottom (fig. 2 main text). Results of direct simulation (fig.7.a) shows clearly that the cloaked region suffers from higher perturbations than the case of a flat bottom (c.f. $-6 < k_s x < 6$ region of fig. 7 here, and fig. 2 of the main text). Also there are interfacial waves left on the downstream ($k_s x > 36$).

There are many ways to compensate for and improve the behavior of our cloaking scheme when the bottom is sloped. A basic improvement is to adjust k_b and n_b according to the mean h_ℓ at the location of each patch. This has been implemented in fig. 7.b. Specifically, the reference depth for calculating the Bragg resonance condition is the depth at the middle of each patch. Clearly the second patch (on the right) has a shorter extent. This is because the

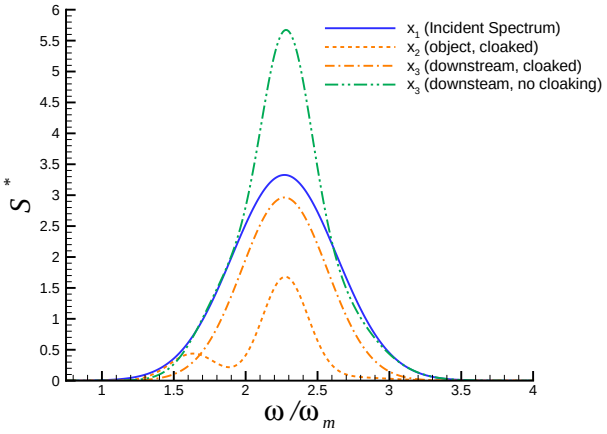

FIG. 5: Cloaking against a spectrum of waves. Plotted curves are the incident wave spectrum (——), downstream spectrum when cloaking present (– · –), downstream spectrum when cloaking is NOT included (— · · —), floating object oscillation spectrum with cloaking (- - -). $\int S^* \mathrm{d}w = \sum_{i=1,5} 1/2(a_i/a_m)^2$. Comparing two plotted curves at x_3 (– · – & — · · —) shows the effectiveness of our cloaking.

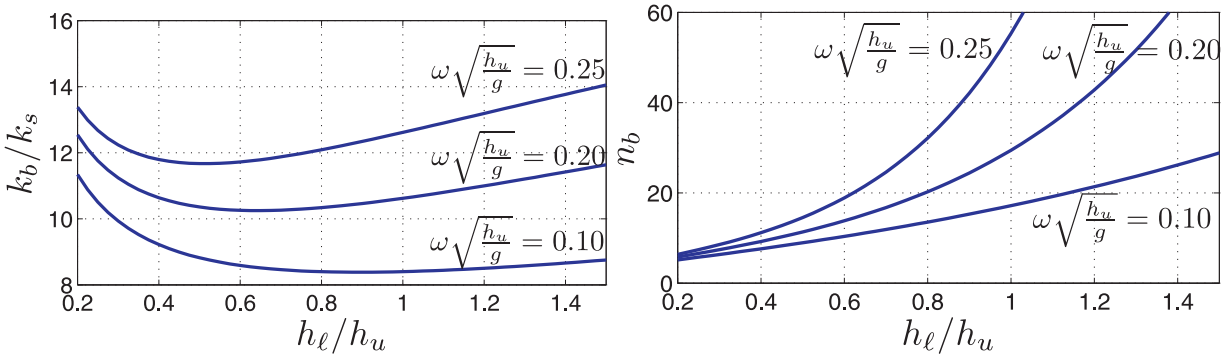

FIG. 6: Effect of the depth of the lower layer on the wavenumber (k_b) and the number of ripples (n_b) that is required to achieve a complete cloaking. (a) Normalized bottom wavenumber (the ratio of k_b/k_s) required for an exact Bragg resonance between surface and interfacial waves is plotted as a function of the ratio of the depth of lower layer to the depth of upper layer (h_ℓ/h_u). Bottom wavenumber is a weak function of the depth of the lower layer, and therefore stays relatively constant over a sloped patch. (b) Number of bottom ripples (needed for a perfect cloaking) as a function of h_ℓ/h_u. As h_ℓ increases (and if the bottom ripple amplitude is kept constant), interaction with the bottom becomes weaker and more ripples are necessary for a complete cloaking. Frequency of incident wave has similar effect on n_b. Note that the strength of a Bragg resonance is a function of $n_b \times a_b$ where a_b is the bottom amplitude. Therefore for a given scenario if n_b is to remain constant, a_b can be varied appropriately to assure all the surface energy goes to the interface over the patch and vice versa.

mean water depth is smaller over the second patch, hence interaction is stronger, and less n_b is needed to transfer a specific amount of energy. Results of direct simulation (fig. 7.b) shows significant improvement in reducing the perturbations in the cloaked region, and less leftover interfacial waves downstream.

[1] S. H. Lamb, *Hydrodynamics* (Dover, 1932).
[2] J. J. V. Wehausen and E. E. V. Laitone, Handbuch der Physik pp. 446–778 (1960).
[3] M.-R. Alam, Y. Liu, and D. K. P. Yue, J. Fluid Mech. **624**, 191 (2009).
[4] M.-R. Alam, Y. Liu, and D. K. P. Yue, J. Fluid Mech. **624**, 225 (2009).
[5] J. B. Pendry, D. Schurig, and D. R. Smith, Science **312**, 1780 (2006).
[6] S. a. Cummer, B.-I. Popa, D. Schurig, and D. R. Smith, Phys. Rev. E **74**, 1 (2006), ISSN 1539-3755.

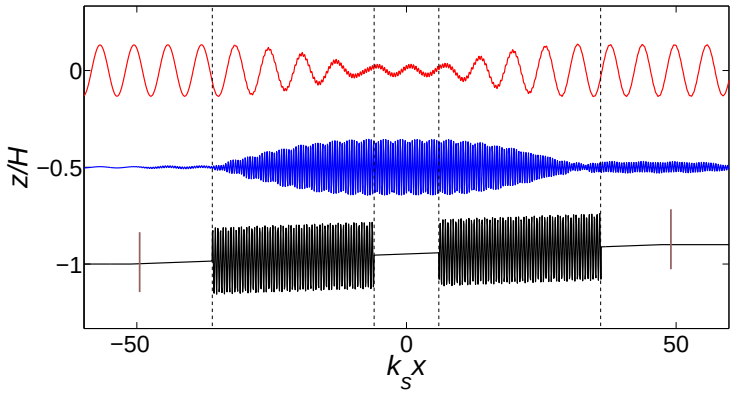

(a)

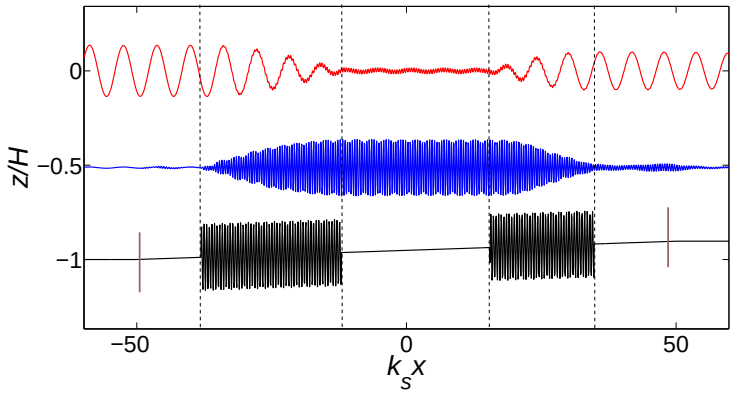

(b)

FIG. 7: Direct simulation for cloaking against a monochromatic surface wave over a sloped bottom. (a) with the same bottom wavenumber and number of ripples as in the case of flat bottom. Specifically $k_b H_0$=4.86 where H_0 is the total water depth before the slope and n_b =62 (fig. 2, main text). (b) with wavenumber and the number of ripples associate with the mean water depth at the location of the patch. Specifically, $k_{b1} H_0$=4.87, n_{b1} =54 and $k_{b1} H_0$=4.88, n_{b1} =41. The performance of cloaking in fig. b is clearly higher than in fig. a. Also the recovery of interfacial wave energy on the downstream is improved in fig. b compared to the not-adjusted values of fig.a. The rest of the parameters are the same as in fig. 2 of the main text.

[7] D. Schurig, J. J. Mock, B. J. Justice, S. A. Cummer, J. B. Pendry, A. F. Starr, and D. R. Smith, Science **314**, 977 (2006).
[8] M. Farhat, S. Enoch, S. Guenneau, and a. Movchan, Phys. Rev. Lett. **101**, 1 (2008).
[9] S. Elgar and B. Raubenheimer, Geoph. Res. Lett. **35**, 1 (2008).
[10] E. Isaacson, Communications On Pure And Applied Mathematics **3**, 11 (1950).
[11] D. Cacchione and C. Wunsch, Journal of Fluid Mechanics **66**, 223 (1974).
[12] C. C. Mei, J. Fluid Mech. **152**, 315 (1985).
[13] P. G. Chamberlain and D. Porter, Journal of Fluid Mechanics **291**, 393 (2006).
[14] Y. Agnon, Physical Review E **59** (1999).